EUROPEAN LABORATORY FOR PARTICLE PHYSICS
LABORATOIRE EUROPEEN POUR LA PHYSIQUE DES PARTICULES

CERN-ST-2000-063
CERN-ST/CV-2000-145/EVC
November, 2000

STUDY OF THE VENTILATION AT ATLAS CAVERN UX15. AIR VELOCITY AND TEMPERATURE AROUND THE MUON CHAMBERS[1]

Emma VIGO CASTELLVÍ

Abstract

The Muon Chambers of ATLAS detector cannot work under temperature differences between two opposed faces above 3 K. In addition, a low velocity of the air around the Muon Chambers is essential to avoid vibration problems. The CV group at the ST division is involved in an airflow simulation inside UX15 cavern to check air temperature and velocity profiles around the ATLAS Muon Chambers. In this paper, the status and the content of the performed theoretical studies will be explained. Three simulation models, which helped to understand the Muon Spectrometer thermal environment and the efficiency of the ventilation system at ATLAS cavern, will be presented. Besides, it will be shown how these studies support the proposal of a deeper individual Muon Chamber study.

[1] Results will be also available on http://evigocas.home.cern.ch/evigocas/atlas_air_flow.html

1 INTRODUCTION

This paper draws a summary of the contributions brought by the ST/CV group in the study of the thermal environment of the ATLAS Muon Spectrometer sub-detector. The temperature difference between opposed faces of the Muon Chambers should not be above 3 K. In addition, a low velocity of the air around the chambers is essential to avoid vibration problems.

The Muon Chambers and the ATLAS cavern ventilation system are first briefly described. Then 3 different models developed with the commercial Computational Fluid Dynamics (CFD) code Star-CD[2] are presented together with the imposed boundary conditions. The resulting temperatures and velocity profiles are shown, focusing on the area around the Muon Chambers.

The aim of the first model is to study the influence of the electronic racks situated on both sides of the ATLAS detector. As the ATLAS experiment is simplified into a big octagon, the model is called the Simplified Octagonal Model.

In the second one, called the Reduced Muon Chambers Model, the Muon Chambers structure is included, but the chambers' size is half their real size. The thermal loads of the electronic racks and the Monitored Drift Tube (MDT) chambers will be taken into account and the results will be compared with those from the first model in which only the electronic racks' thermal load is considered.

The geometry of the third model, the Large Muon Chambers Model, corresponds to the real Muon Spectrometer disposition. Two simulations were performed with this model: the first includes the same thermal loads as for the Reduced Muon Chamber Model and, in the second, all the thermal loads inside the UX15 and ATLAS detector are considered.

Finally, some general conclusions will be given.

2 THE MUON SPECTROMETER

The Muon Spectrometer is the outer sub-detector of the ATLAS experiment (see Figure 1). Its main task is to identify and measure muons coming from LHC interactions at point 1 (ATLAS). In particular it will be responsible of determining their signs and momenta with a high precision even at the highest luminosities.

For a good performance of the sub-detector, each Muon Chamber should not stand a temperature difference between two opposed faces larger than 3 K.

Another important parameter for their operation is the velocity of the air surrounding the chambers. High velocities could produce vibrations on the MDT's, that would act as sails.

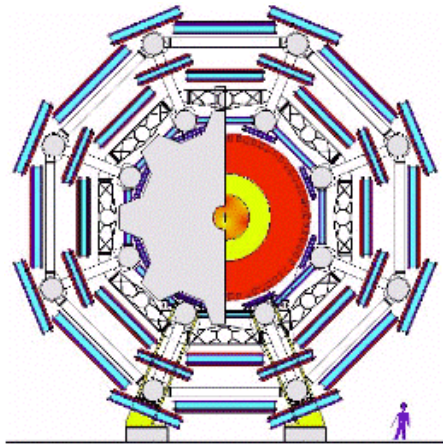

Figure 1: frontal view of the Muon Chambers

[2] Star-CD is a CFD code supplied by Computational Dynamics Ltd., United Kingdom.

2.1 Nomenclature and Co-ordinate System

The Muon Spectrometer co-ordinate system is a right-handed system with the z-axis being the beam axis, the y-axis pointing upwards, and the x-axis pointing towards the centre of the LHC ring [1]. The LEP experiments and the other LHC experiments also use this system.

Within the Muon Spectrometer the following nomenclature is used.

- **Region:** two regions are distinguished**,** barrel (B) and end-cap (E).
- **Station:** location of a chamber or a group of chambers. The whole sub-detector consists of 3 layers or stations of Muon Chambers, the inner (I), the middle (M) and the outer (O).
- **Sector:** the system is subdivided into 16 sectors; they are numbered from 1 to 16. A sector corresponds to an azimuthal area defined by the barrel magnet structure. Sector boundaries are not sharply defined, they correspond to the azimuthal regions between barrel coils (odd sector numbers) and those covered by the barrel coils (even sector numbers). The x-axis (ϕ=0) crosses sector 1; see Figure 2. Sectors are counted clockwise when looking from the interaction point towards the +z direction and counter-clockwise when looking towards the –z direction.

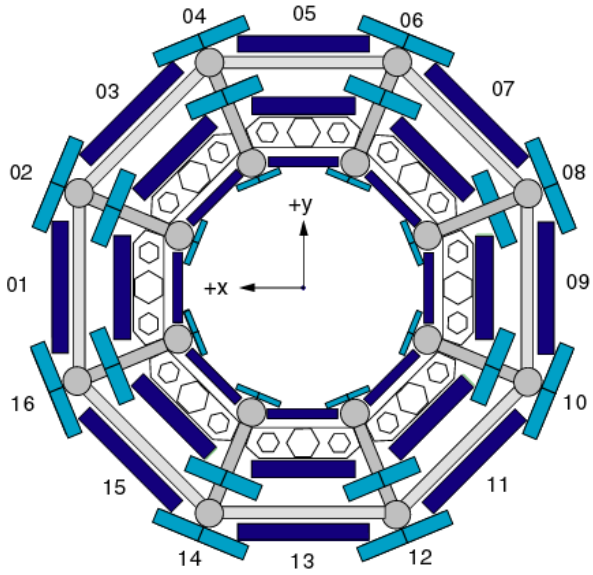

Figure 2: The co-ordinate system and sectors of the Muon Spectrometer

The chambers in the odd sectors being wider than the ones in the even sectors. They are referred to as large (L) and small (S), respectively.

Since the chamber geometry is closely linked to the location of the chamber, a chamber naming system has been introduced. It follows this pattern: XXXY. Individual chambers or groups of chambers with similar characteristics are thus easily identified.

- X: describes the chamber type and global location:
  - X_1 : Region (B = barrel, E = end-caps, F = forward);
  - X_2 : Station (I = inner, E = extra, M = middle, O = outer);
  - X_3 : L = large or S = small.
- Y: Sector number (01–16).

For the current study the inner Muon Chambers (BIS and BIL) will be considered as MDT's (single tubes layers); the middle ones (BMS and BML) as MDT's with one RPC (gas gaps) on each

side; and the outer chambers as MDT's with one RPC on one side (inner one for BOS, outer one for BOL).

2.2 The Thermal Loads[3]

The Muon System

The MDT's have heat-dissipating electronics on one of its short sides that will be taken into account for the simulation.

The relevant thermal loads included in the calculations are summarised in Table 1. The values are expressed in watts per unit of surface (the surface is oriented in the rz plane, where r is the radius in the ATLAS cylindrical co-ordinate system).

Table 1: Thermal loads on the chambers

Muon Stations	*Thermal Load (W/m^2)*
BOS, BOL	15.46
BML	13.56
BMS	15.3
BIS	35.46
BIL	24.04

As it was said before, the RPC's are gas gaps situated at the inner and outer sides of the BML and BMS chambers, at the outer side of the BOL chambers and at the inner side of the BOS chambers. Their associated electronics are estimated to dissipate 4.8 W/m^2.

Electronic racks

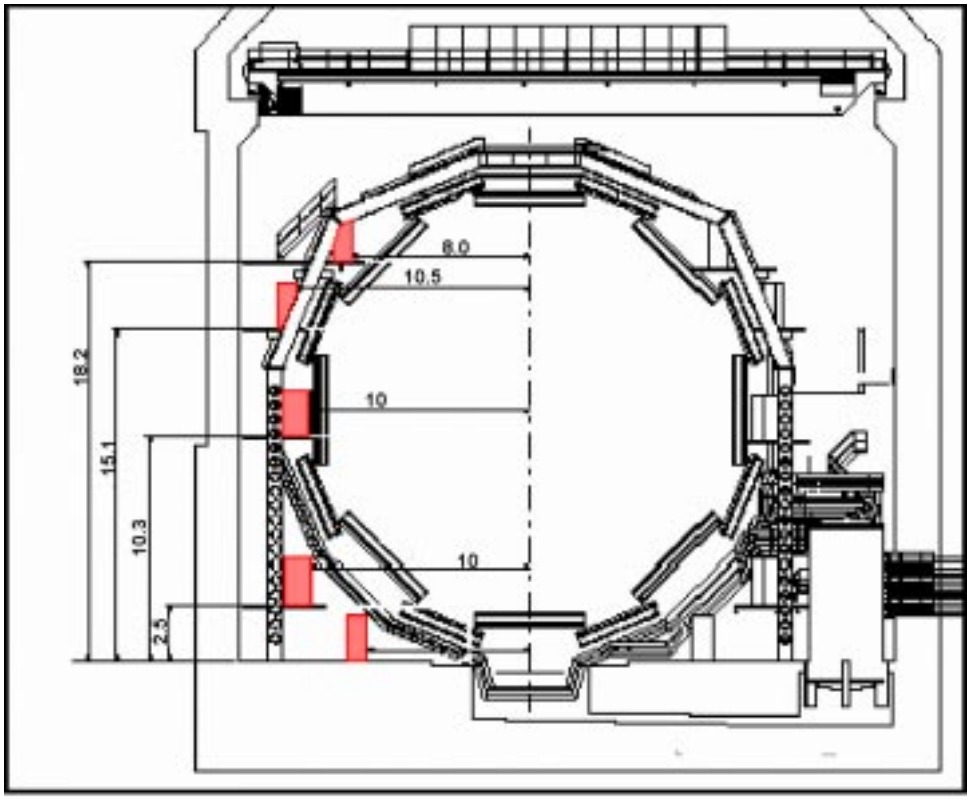

Figure 3: Location of racks [2]

[3] All thermal loads are given in W/m^2, which is the unit used by StarCD for the computations

There are 5 lines of electronic racks on each side of the experiment. The racks will be considered to be 900x2000 mm^2 in the xy plane. Their locations can be seen on Figure 3.

The racks have a thermal load of 3.45 W/m^2 on the 4 surfaces perpendiculars to the xy plane.

The Barrel Coils

There are 2 barrel coils in each of the 8 even sectors (see Figure 2). They are assumed to be heat sinks of -3.98W/m^2.

The Calorimeters and Inner Detector

The inner detector dissipates heat mostly in the gaps.

Recent results for heat dissipation in the tile calorimeter and liquid argon calorimeter confirm the assumption of 90% efficiency of the cooling systems of the tile calorimeter. Under these assumptions, the total heat dissipated at the surface of the tile barrel calorimeter is 8W/m^2.

Thermal loads for each simulation

The thermal loads considered for each model are listed in Table 2

Table 2: Thermal loads in W/m^2

Model	***Simulation 1*** *Simplified Octagonal*	***Simulation 2*** *Reduced Muon Chambers*	***Simulation 3*** *Large Muon Chambers (1)*	***Simulation 4*** *Large Muon Chambers (2)*
ATLAS experiment	41.8			
BOS, BOL		15.46	15.46	15.46
BML		13.56	13.56	13.56
BMS		15.3	15.3	15.3
BIS		35.46	35.46	35.46
BIL		24.04	24.04	24.04
Electronic Racks	3.45	3.45	3.45	3.45
RPC				5
Tile Barrel Calorimeter				8
Barrel Coils				-3.98

3 VENTILATION

The air is supplied into the ATLAS cavern, called UX15, through 12 vertical inlets situated close to the wall at the bottom of the hall. It is evacuated by means of 2 extraction points, one at the top of the UX15 and another one sitting in the pit at the bottom of the cavern. Their locations are shown in Figure 5.

For the Simplified Octagonal and Reduced Muon Chamber Models, the nominal air flow rate accounts for 45,000 m^3/h. The velocity of the air at the face of the 12 vertical supply units is then 0.52 m/s.

During the progress of this analysis, the nominal air flow rate was increased to 60,000 m^3/h in order to match an increased dissipation from the ATLAS detector [3]. The area of the supply units was also modified, what made the velocity at their face decrease to 0.31 m/s. This values were considered for the study of the Large Muon Chamber Model.

The ventilation parameters included in the analysis of each model are listed in Table 3.

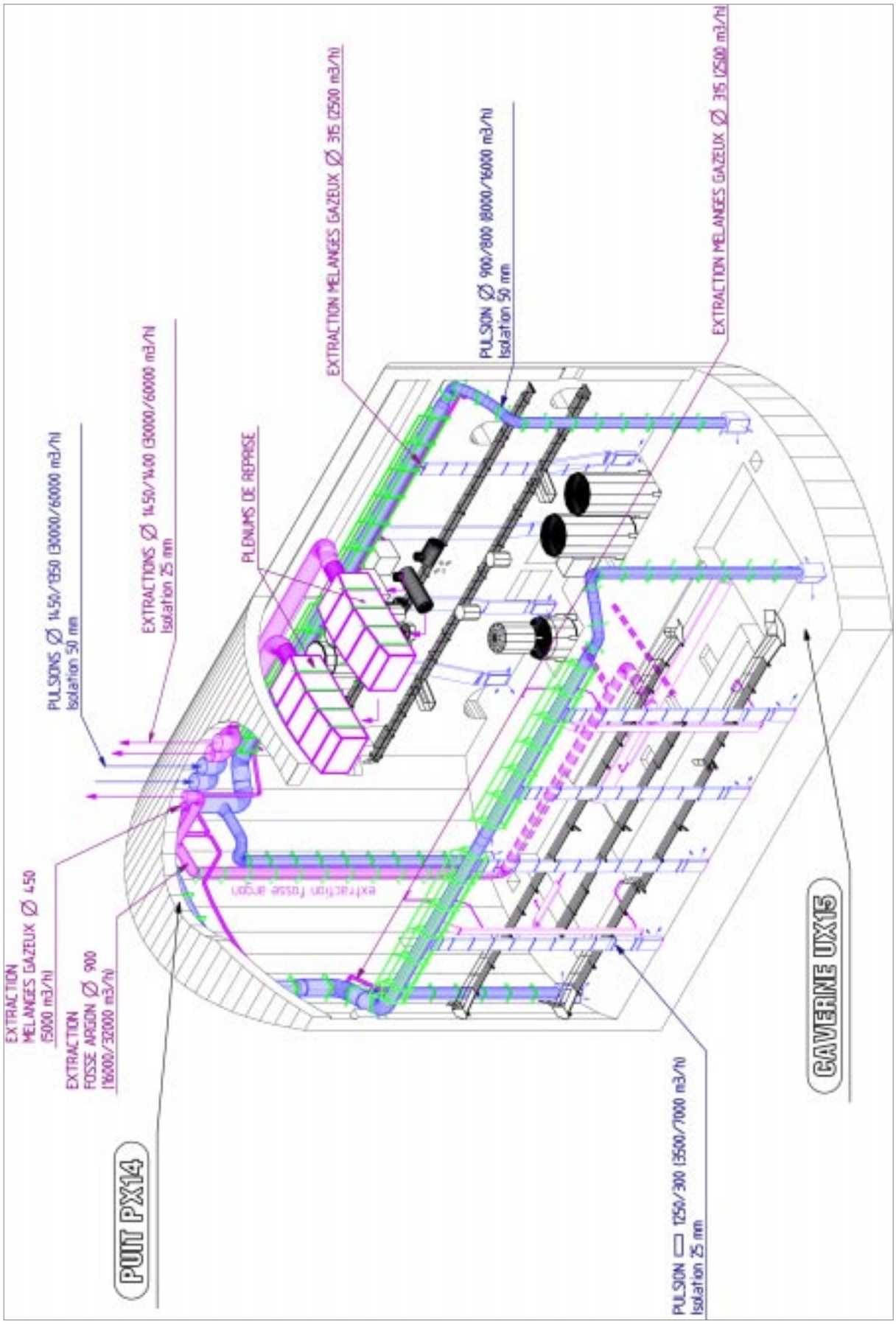

Figure 4: General view of ventilation systems at UX15

Table 3: Ventilation parameters

Model	***Simulation 1*** *Simplified Octagonal*	***Simulation 2*** *Reduced Muon Chambers*	***Simulation 3&4*** *Large Muon Chambers (1 and 2)*
Air flow rate (m^3/h)	45000	45000	60000
Inlet velocity (m/s)	0.52	0.52	0.31
Inlet air temperature (°C)	17	17	17
Flow extracted by the upper unit (%)	68	68	78.95
Flow extracted by the unit in the pit (%)	32	32	21.05

4 GENERAL ASSUMPTIONS

The determination of the air temperature and velocity fields in and around an object as complex as the ATLAS experiment in its cavern with a detailed 3D model of its geometry, different heat sources and boundary conditions, requires computing facilities out of hand. Taking advantage of the repetitive geometry and boundary conditions in the longitudinal direction, the problem has been simplified and analysed in 2D.

The calculated model is a cross-section with two coincident inlets (one on each side of the detector, see green arrows on Figure 5), one extraction at the top of the UX15 and another at the cavern bottom pit (see blue arrows on Figure 5).

Regarding the heat exchange mechanisms, only conduction through the air, and forced and natural convection have been considered. The radiation effect was disregarded for the 3 treated models. A short calculation was made to support this decision: the radiative heat flow between two muon chambers was approximated to that between two infinite parallel surfaces. The material properties used were those for aluminium. The results showed that the heat exchange resulting from the calculation was two orders of magnitude smaller than the heat load dissipated by the Muon Chambers or by the electronic racks.

5 SIMPLIFIED OCTOGONAL MODEL

5.1 Assumptions

For the first study, the whole ATLAS experiment has been considered as an octagon inside the UX15 cavern walls. The total thermal load for the detector is estimated to be 100kW, distributed on its surface.

Only the electronic racks are kept outside this structure. The racks are represented by their outer surfaces with thermal boundaries on them. The model is shown in Figure 5.

The aim of the simulation is to study the global influence of the ATLAS detector and, particularly, of the electronic racks, on its environment inside the cavern.

5.2 Results

Figures 6 and 7 show the velocity and temperature maps resulting from the calculations on the first model.

Because of natural convection, a significant ascending flow can be seen along the detector's wall and up to the top of UX15. It can also be observed a high velocity zone between the two first

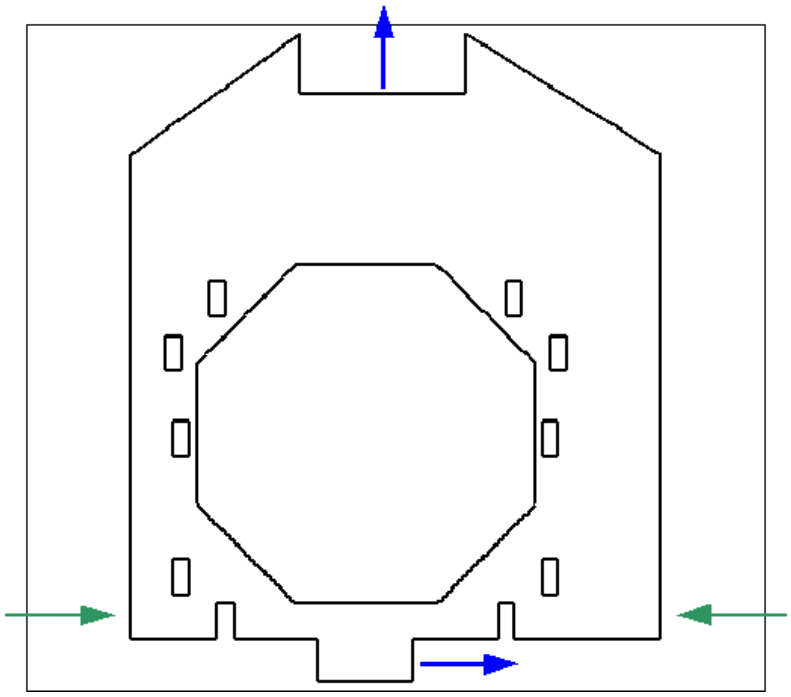

Figure 5: The 2D Simplified Octagonal model

racks at the bottom of the cavern, on both sides of the experiment. This is due to the forced air extraction on the near bottom of the UX15 hall, which also implies high velocities through this outlet.

Regarding the temperature distribution, there is almost a difference of 3 K between the inlets and the top outlet. There are no significant hot points around the electronic racks, but they exist on the bottom side of the octagon and especially on the top side of the octagon. On the upper half of the hall, the temperature distribution and, in particular, the chimney effect on top of the octagon, show clearly the influence of natural convection.

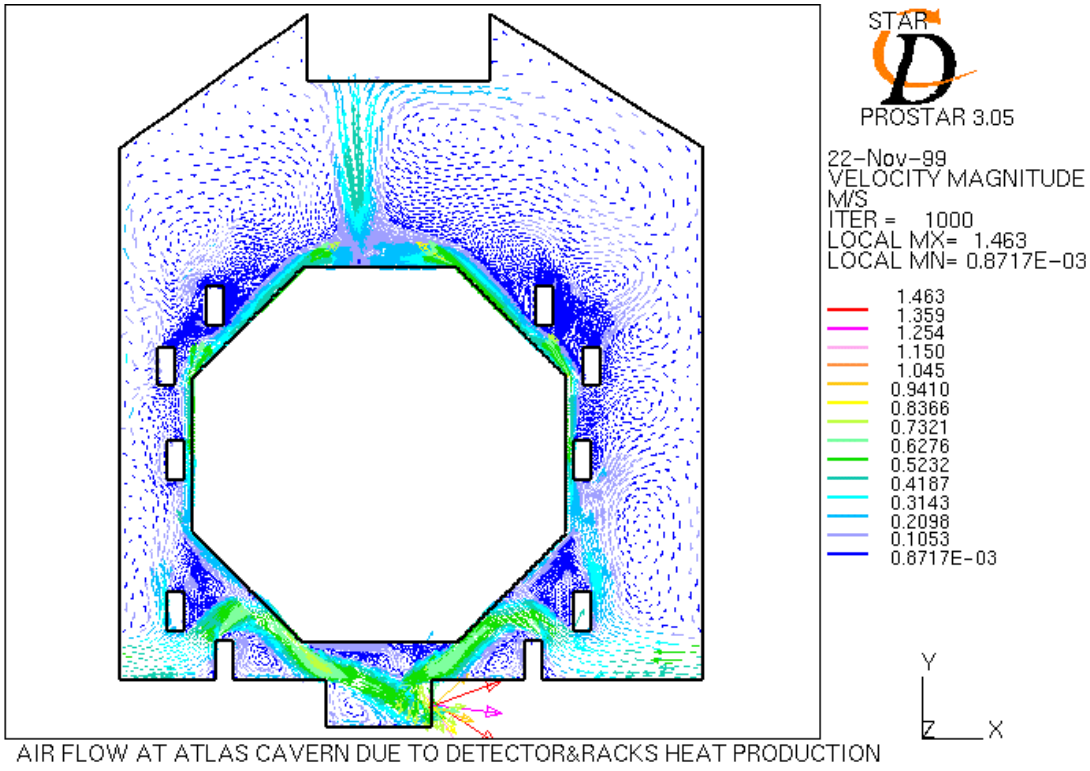

Figure 6: Velocity distribution, Simplified Octagonal model

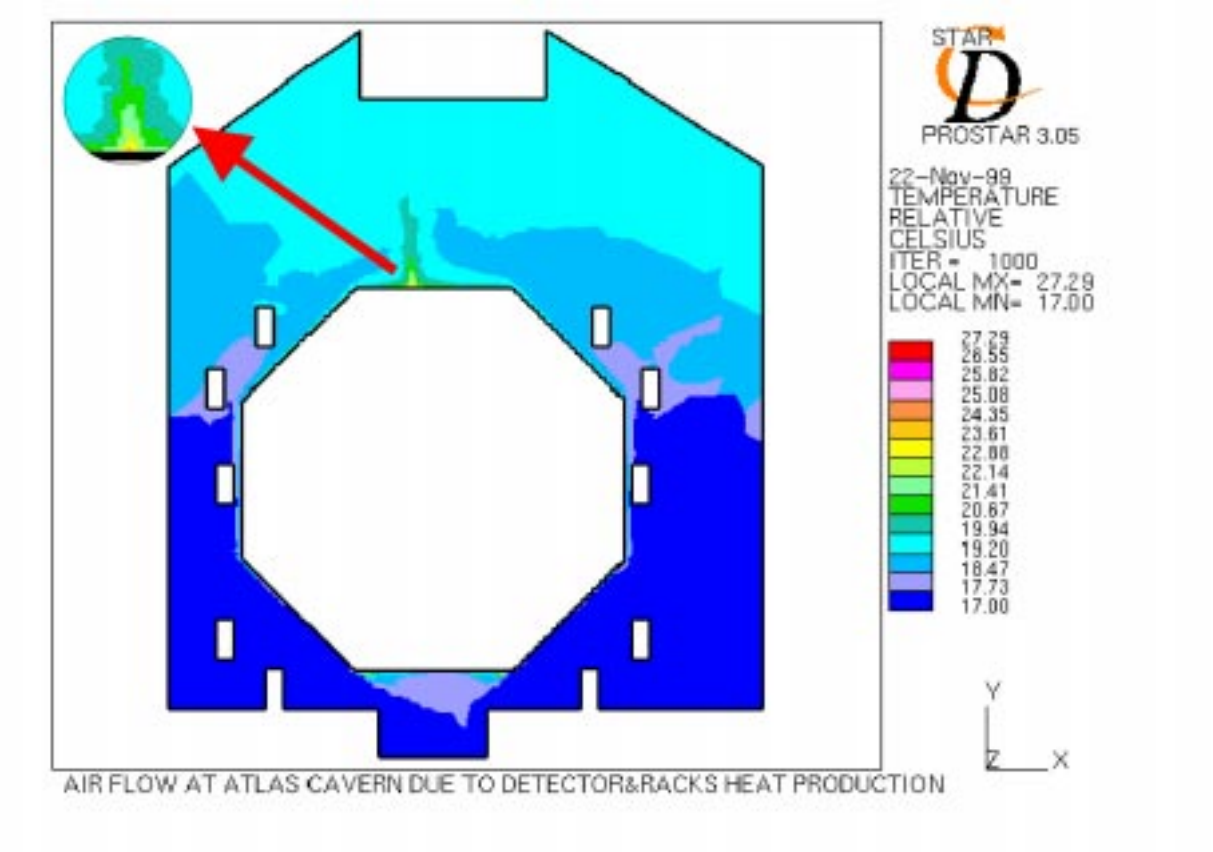

Figure 7: Temperature distribution, Simplified Octagonal model

6 REDUCED MUON CHAMBERS MODEL

6.1 Assumptions

The second model is also taken from a cross-section with two coincident inlets (one on each side of

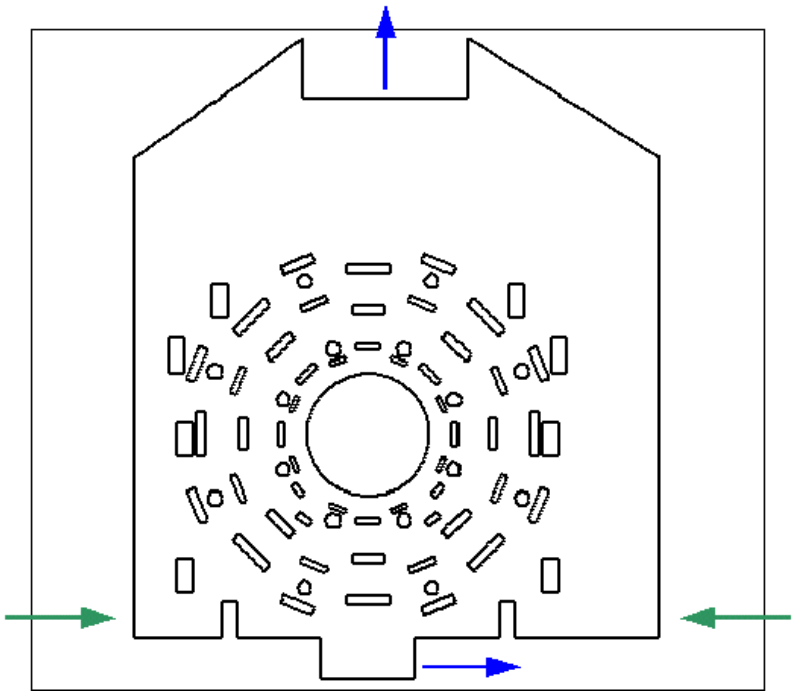

Figure 8: The Reduced Muon Chambers model

the detector), one extraction at the top of the UX15 and another one in the pit at the bottom of the cavern.

The Reduced Muon Chambers Model differs from the previous one in the modelisation of the ATLAS experiment. The Muon Spectrometer is represented detailing each type of chamber. Also the Barrel coils' geometry is taken into account. The calorimeters and the inner detector are represented as a circle and the racks remain as they were. This model can be seen in Figure 8. The green arrows point to the inlets; the blue ones point to the outlets.

In this second model, the length of the Muon Chambers has been reduced to half its size to increase the gaps between the chambers. The goal is to avoid the divergence of the calculations because of instabilities of natural convection and the narrow free spaces between some of the chambers.

The aim of this second calculation is to study the influence on the Muon Chambers thermal environment of both the MDT's electronics and the electronic racks.

6.2 Results

Figures 9 and 10 show the distributions of velocity and temperature resulting from the calculations on the second model.

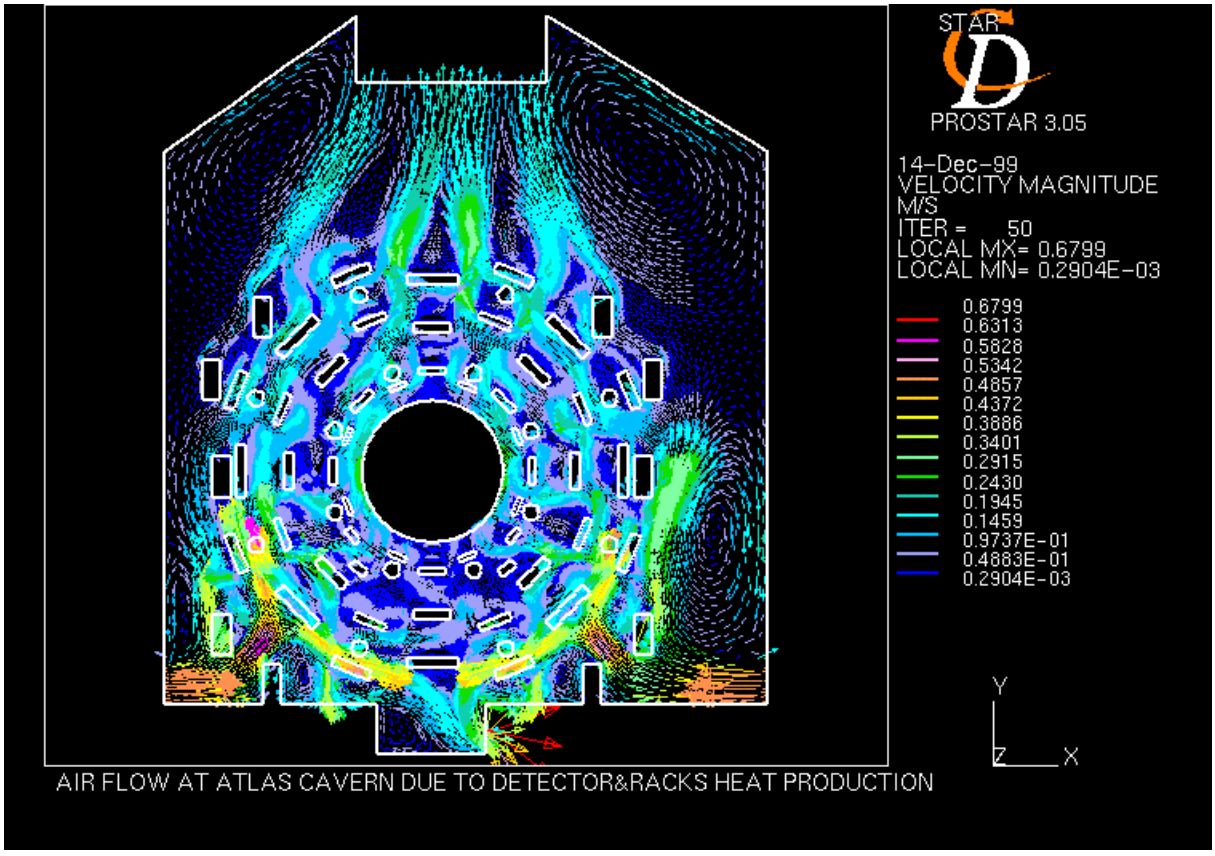

Figure 9: Velocity distribution, Reduced Muon Chamber model

The air flowing between the chambers together with the effect of natural convection increases the number of vortices. This makes the velocity map less uniform than in the previous model. The higher velocity distribution is located in the area comprised between the ventilation inlets, the lower part of the detector and the bottom pit. That is again due to the forced air extraction on the near bottom of the UX15 hall, and also due to the impact of the incoming flow against the outer chambers on sectors 12 and 14.

The temperature difference between the bottom and the top of the cavern is due to the buoyancy in the air when flowing through the chambers. In this computation, the total heat load is

smaller than in the previous one because neither the RPC's nor the inner detectors or the barrel coils were considered. The maximum temperature is therefore lower in this case and accounts for 21.50°C. The hottest points are located on the electronics side of some inner chambers.

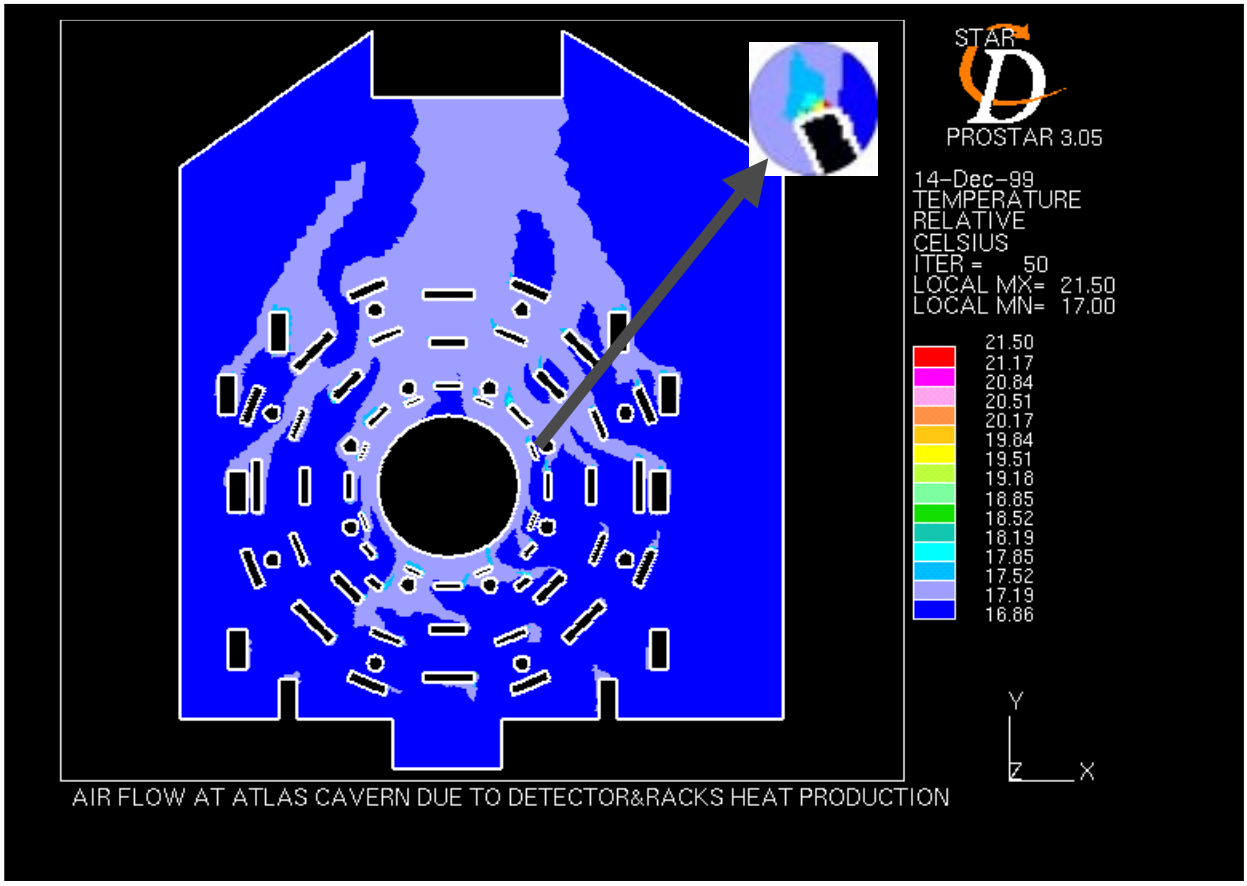

Figure 10: Temperature distribution, Reduced Muon Chamber model

7 LARGE MUON CHAMBERS MODEL

7.1 Assumptions

The Muon Chambers have been enlarged to their real length. However, the BIS and BIL chambers widths have been reduced of 40mm and 50mm respectively to ease convergence. With the same objective, the radius of the Tile Barrel Calorimeter has been reduced from 4.24 m to 4.0 m and the radius of each Barrel Coil from 0.583 m to 0.500 m.

The Large Muon Chambers model is shown in Figure 11. The green arrows point to the inlets; the blue ones point to the outlets.

The aim of this third calculation is to study the influence of the narrow air paths between the different types of chambers on the Muon Chambers thermal environment.

7.2 Results for Large Muon Chamber (1)

In general, air velocity values around the ATLAS cavern have decreased due to a slower ventilation inlet. In addition, the high air velocities at the bottom of the cavern are also affected by the less important extraction at the pit. Anyway, the area between the inlets, the two first racks and the lower part of the detector remain with quite high velocities. On the other hand, the velocity of the air surrounding the chambers, in relation to the inlet velocity, is higher than in previous studies as a result of the narrow paths between the various chambers. That is especially true for the top part of the

detector because the increase of the extraction power at the top of the UX15 produces a forced flow through it.

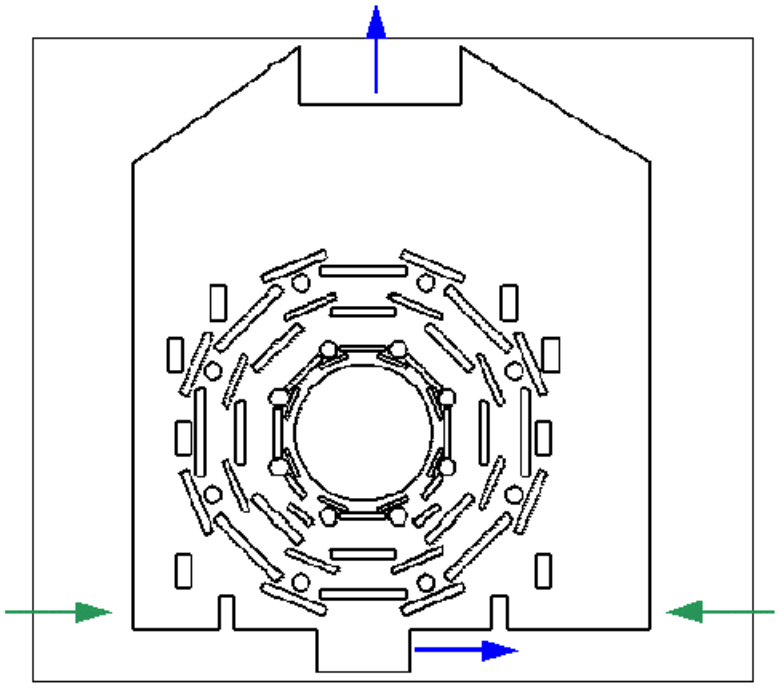

Figure 11: The Large Muon Chambers model

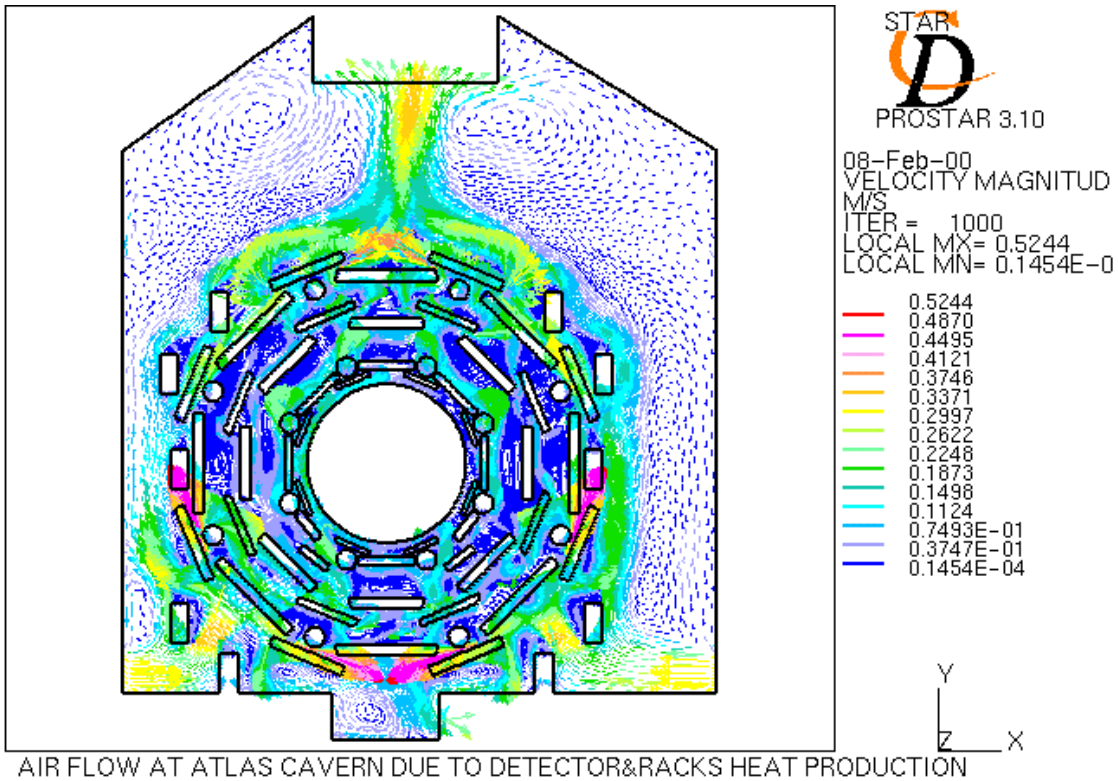

Figure 12: Velocity distribution, Large Muon Chamber model

Regarding the temperature distribution, there is only a difference of 1 K between the inlets and the top outlet. The hottest points are again located on the electronic side of some inner chambers. On the top half of the hall the temperature distribution shows clearly the influence of natural convection with a significant chimney effect.

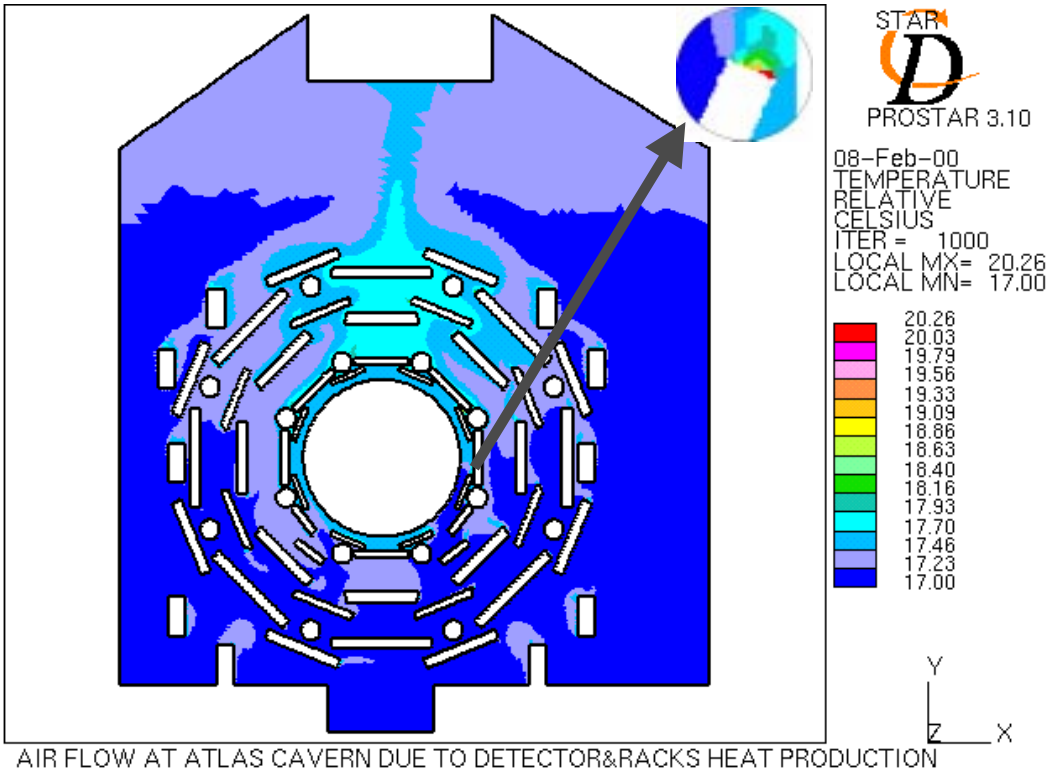

Figure 13: Temperature distribution, Large Muon Chamber model

7.3 Large Muon Chamber (2)

To conclude the study of the air velocity and temperature around the ATLAS Muon Chambers, a second simulation has been done using the Large Muon Chamber Model. We will call it Large Muon Chamber (2).

What differentiates this simulation from the previous one, is the inclusion of all the thermal loads in the calculation. This means taking into account the heat loads of the RPC's electronics, the Tile Barrel Calorimeter, the inner detector and the Barrel Coils. The RPC heat dissipation will be considered on each of the long sides for the BML and BMS chambers, on the outer side for the BOL chambers and on the inner side for the BOS chambers. For the Tile Barrel Calorimeter and the Barrel Coils, the thermal load is distributed on their lateral surface (on the direction z).

The results of this variant can be seen in Figures 14 and 15. The velocity distribution hardly varies, with more vortices probably due to a stronger free convection effect than in the previous simulation.

The vertical temperature difference across the cavern becomes 2 K because of the new thermal loads considered. The most important result from this simulation is the temperature gradients between the faces of the Muon Chambers. The maximum temperature difference between air at both sides of a muon chamber is 4.1°C, as it happens at BOL13. The hot spots, around 23°C, are located on the electronics side of the inner chambers and on the long sides of the upper middle chambers.

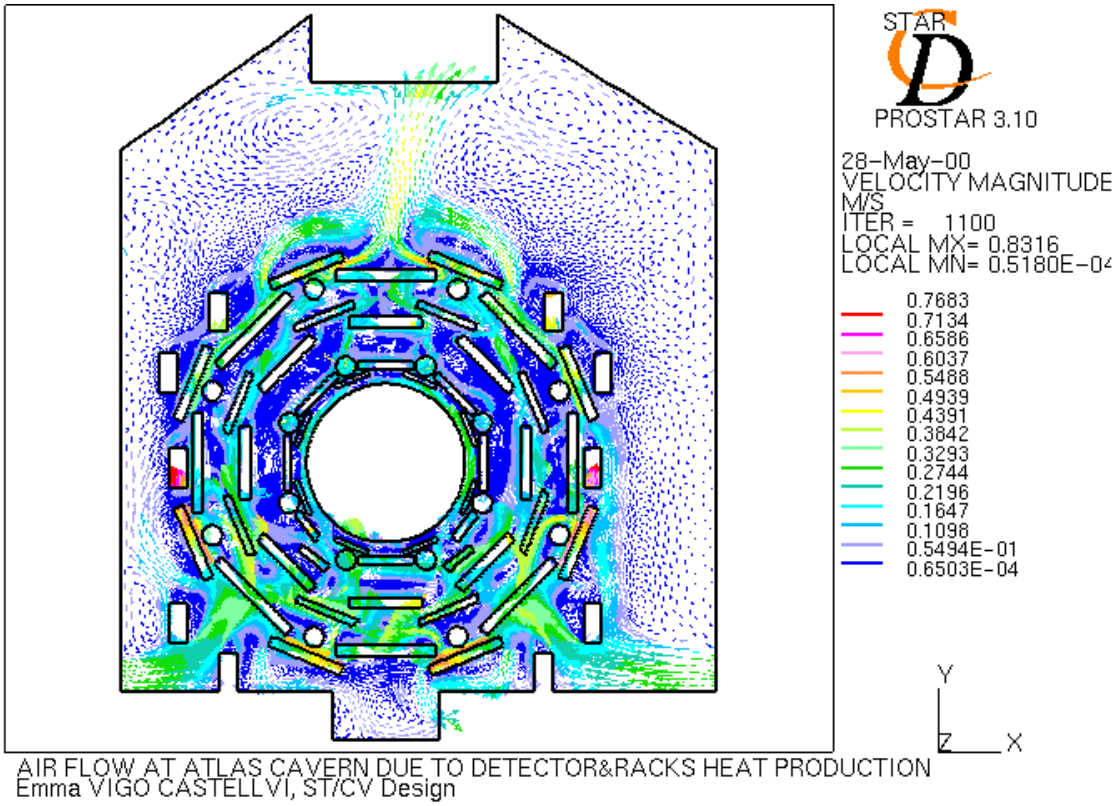

Figure 14: Velocity distribution, LMC2 model

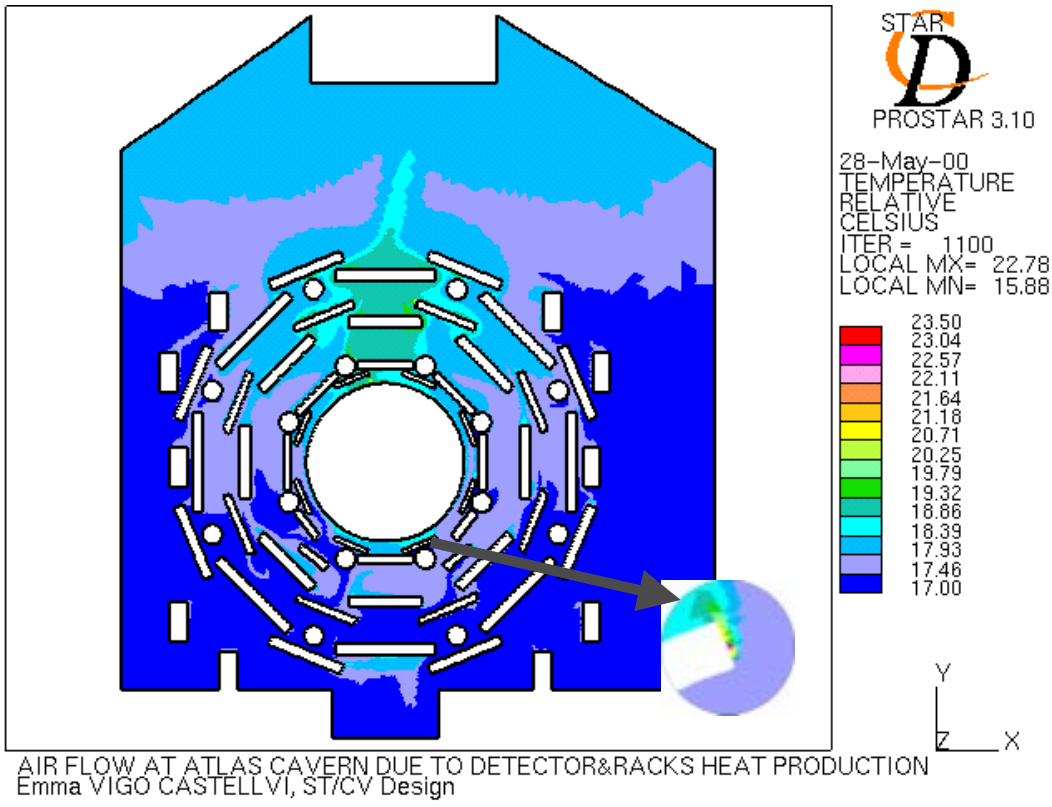

Figure 15: Temperature distribution, LMC2 model

8 CONCLUSIONS

This paper described the different steps leading to a realistic model using the StarCD computational-fluid-dynamics code. The simulations take into account air movement caused by forced and natural convection around the Muon Spectrometer of ATLAS. The results give a global understanding of the heat distribution around the Muon Chambers and the evolution of air velocity.

The heat load coming from the electronic racks have only minor influence on the thermal environment of ATLAS detector. The main influence on the temperature map and air velocity distribution around the Muon Chambers sub-detector comes from the MDT's and RPC's thermal loads.

The computed velocities do not attain high values, what should avoid structure vibrations.

The calculations show that the maximum temperature difference between chambers' faces could go beyond 3°C (4.1°C is reached in BOL13 Muon Chamber) and hence could cause deformations in the structure.

Therefore it would be advisable to perform a simulation considering the Muon Chambers as solids to study the thermal behaviour across them. Unfortunately this model cannot be carried out together with the whole UX15 cavern due to the too big difference between the cavern and the Muon Chambers dimensions.

For this reason, a proposal for the next step is a more detailed study taking into account the different elements and materials of the muon chambers structure. The model would consist of an individual muon chamber and the boundary conditions (heat transfer coefficient and air temperature at surface) would be taken from the results of the simulation Large Muon Chamber (2). The ANSYS code or similar is proposed for the calculation, as the simulation will consist of a solid model treating a purely conductive problem.

References

[1] 3rd Chap. "Naming and Conventions" of the Muon Spectrometer TDR

[2] ATLAS Thermal Calculations Third Iteration Specifications - document ATC-T-ES-0001

[3] New boundary ventilation conditions - document ATC-GE-EM-0043, Jean Roche

Acknowledgements

I would like to thank my colleague Daniel GASSER for our useful discussions on CFD software and fluid-thermodynamics.